ACS OMEGA

http://pubs.acs.org/journal/acsodf

Article

Application of Silicomanganese Fume as a Novel Bridging Material for Water-Based Drilling Fluids

Waseem Razzaq, Salaheldin Elkatatny,* Ahmed Gowida, and Ariffin Samsuri

Cite This: *ACS Omega* 2023, 8, 509–518

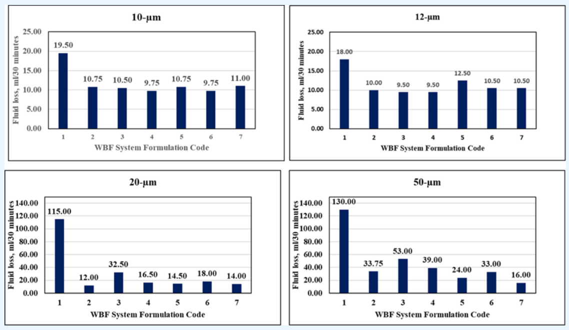

ABSTRACT: Steelmaking industrial waste, that is, silicomanganese fume (SMF), is one of the byproducts obtained during the steelmaking process in an electric submerged arc furnace at 1500 °C. Millions of tons of such wastes are generated yearly and used in different applications such as road construction, cement mortar, recycling into sinter plant, and so forth. In this study, the application of SMF in the drilling operations was investigated by employing SMF as a bridging material (BM) in water-based drilling fluid (WBF). The SMF samples were collected and dry-sieved, and then, the retained particles on each mesh were examined for elemental analysis. Thereafter, a battery of tests was performed using the WBF-SMF system comprising different SMF grades and mixed grades to investigate their bridging performance. The commercial BM (marble) was used as a reference fluid (WBF-marble system) for comparative investigation. The bridging performance of WBF-SMF and WBF-marble systems was tested and compared at 190 °F and 300 psi testing conditions using 10, 12, 20, and 50 μm ceramic discs. The processing techniques have shown that raw SMF does not require prolonged processing steps like the other waste material requires. All the SMF grades have shown homogenous chemical composition in oxides of manganese, silicon, sulfur, calcium, magnesium, and iron. Moreover, the WBF-SMF system have shown substantial improvement in bridging and sealing performance with average 47, 42, 84, and 75% superior fluid loss performance against 10, 12, 20, and 50 μm ceramic discs, respectively, compared to the WBF-marble system. While comparing the filter cake thickness, the WBF-SMF system has deposited a filter cake with more than 50% reduction in thickness compared to the WBF-marble system for different ceramic-disc sizes. Consequently, this study has introduced SMF as a novel BM with a unique particle size distribution that can be used in WBFs to plug formation pores effectively. In addition, this waste material (SMF) has been investigated as an economical, effortless, readily available, and high-performance material compared to other commonly used BMs.

1. INTRODUCTION

Silicomanganese (SiMn) is a ferroalloy being used in the steelmaking industry to provide silicon (Si) and manganese (Mn) for high strength steelmaking.[1] During the entire steelmaking process, several byproducts are generated such as blast furnace slag, steelmaking slag, fly ash, blast furnace clarifier sludges, blast furnace flue dust, mill scales, waste refractories, coke breeze, and silicomanganese fumes (SMFs).[2] The silicomanganese is one of them and known in the literature as SMFs.[3−8] The SMF is reported by several other researchers as a byproduct of the steelmaking industry.[6,9,10] In Spain, waste generation of the steelmaking industry is 15 to 20% of the production.[11] In European Union, 22 million tons of slags were generated in 2010, and the majority of the waste generated was utilized as a landfill.[12] Other applications of steelmaking waste include road construction,[13] cement mortar,[6] and recycling into sinter plant.[14] So far, none of the prior studies have investigated the particle size distribution (PSD) of SMF and its bridging and sealing ability in drilling fluids.

Drilling fluids are a blend of natural and synthetic chemicals added into a base carrier fluid to facilitate drilling downhole for hydrocarbon extraction.[15] Drilling fluids are essential components of drilling operation that helps the driller to achieve intended depth. The function of drilling fluids is to provide hole cleaning, bit cooling, and lubrication, maintain hydrostatic head pressure, suspend cuttings under quiescent conditions, and deposit a filter cake (FC).[16] Deposition of effective FC or filtration properties of drilling fluids should be maintained in the laboratory within the guidelines mentioned by the American Petroleum Institute (API). If the filtration properties are not maintained properly, a number of challenges are going

Received: August 24, 2022
Accepted: December 6, 2022
Published: December 23, 2022

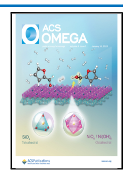

https://doi.org/10.1021/acsomega.2c05456
ACS Omega 2023, 8, 509–518

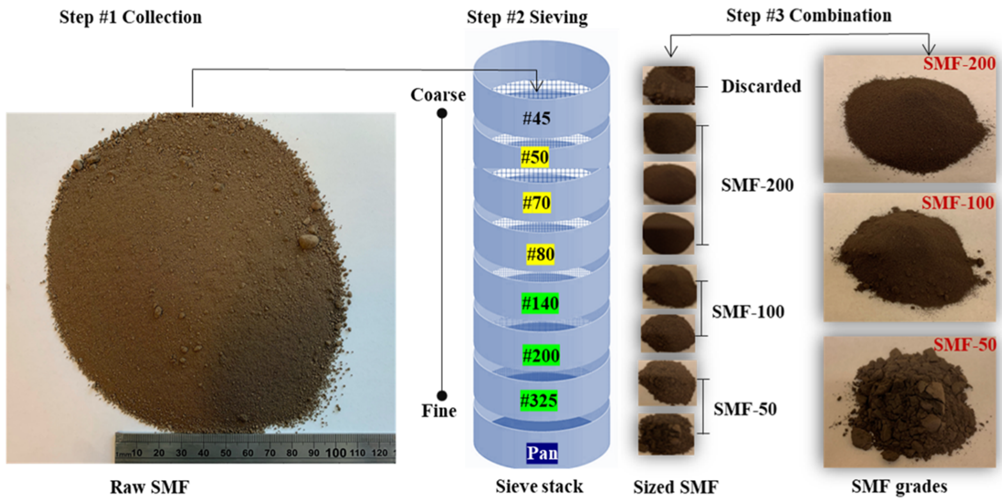

Figure 1. Processing steps of " raw" SMF waste material into SMF grades.

to be encountered while drilling the well, such as high filtrate or sometimes loss of drilling fluid into the subterranean formation, and depositing a thick mud cake.[17] Ultimately, these factors commence circulation lost and/or stuck pipe challenges. Certain types and sizes of solid materials are added into the drilling fluid to bridge the pore throats of the exposed subterranean formation.[18] At the formation face, due to the pressure overbalance of the drilling fluid, two mechanisms occurred. The liquid phase of the drilling fluid passes through these formation pores (known as filtrates), and then, solids of the drilling fluid bridge the formation of the pore throat and deposit a FC.[19] This FC deposited on the formation face acts as an impermeable layer to stop fluid migration from wellbore to formation and vice versa.[20]

The deposition of FC and fluid loss (FL) mechanism was explained in the classical FL theory formulated by Howard and Fast in 1970.[21] The theory demonstrates that the FL and FC deposition occurs in several stages. In the first stage, formation fluid is displaced by the liquid phase of the WBF system due to hydrostatic head pressure. This is followed by plugging the formation pores with large particulates that deposit internal FC. Lastly, the formation of external FC occurs on the surface of the wellbore walls. Navarrete et al. (1994) have further iterated that internal FC controls the FL, as it bridges the pores and pore throat of the formation with larger sized particles.[22] If the particles present in the active WBF system are much smaller than formation pore size, then these particles are likely to penetrate into the formation with the initial FL. However, if multimodal or different particle sizes are present in the mud system, then bigger particles chock the pore throat and finer particles deposit afterward to completely plug the formation pores.[23]

Darley, in 1965, has explained the bridging mechanism occurring in three steps.[23] In the first step, during the phase of displacing formation fluid with filtrate volume, the super-fine particle passes through the formation pores and creates initial resistance. This phenomenon is also referred to as spurt loss, which is further defined as "passing of super fine particle in conjunction with base fluid through formation pores until its pores become bridged". Generally, it takes 1−2 s and very small amount of filtrate volume penetrates the formation pores during the spurt loss phenomenon. In the second step, the larger sized particles bridge the pores. The medium- and small-sized particles fill the gaps and reduce the filtrate volume, thus working as the packing mechanism. In the third step, finer size particles further seal the formation pores.

The material that has been used in the industry to plug the pores are known as bridging materials (BMs) or lost circulation materials and they are flaky, granular, fibrous, blended, acid-soluble or degradable, hydratable or swellable, and nanoparticles.[24] The overall cost of drilling fluid additives is increasing every year, and statistics showed that oil and gas organizations spent multibillion US dollars to acquire additives.[25] Research and development attempts have been made among academia, service, and operator companies to minimize the drilling fluid cost. Recent trends in the literature have revealed that researchers are putting efforts to investigate economical materials such as the waste material from diverse origins and explore their application as a drilling fluid component, that is, BM or loss circulation material. The example of such research studies includes waste date seed powder,[26] shredded waste car tyres,[27] deceased date tree waste,[28] date tree trunk,[28] banana peel,[29] powered grass and grass ash,[30] Styrofoam waste,[31] durian rind,[32] sunflower seed and orange powder,[33] seashells,[34] eggshell,[35] potato peels and mandarin peels and other household wastes,[36,37] date tree ARC ECOFiber,[38] oil palm trunk waste,[39] carton waste,[40] and Eucalyptus bark powder waste.[41]

Though the abovementioned materials are considered as economical materials due to their origin as a waste of other industries, these materials require several processing steps. The common processing steps used to convert waste into BM includes the collection of the waste material from the production site, drying at several steps—to remove moisture, washing—to extract clean waste, boiling—in case of seashell, shredding and removing steel wires—in case of tyres, grinding to breakdown larger pieces or particles, sieving—to acquire proper particle size, and finally packing as an end product. Other significant factors that are required to process waste materials into the final product are temperature and time for removal of moisture before the final step. For instance, in Medved et al., 2022 articles, mandarin peel waste was successfully converted into water-based drilling additives by performing several processing steps.[42,43] These steps include collection of mandarin peel from waste, oven drying at 90 °C for 48 h, additional drying for 24 h, grinding, and sieving

https://doi.org/10.1021/acsomega.2c05456
ACS Omega 2023, 8, 509−518

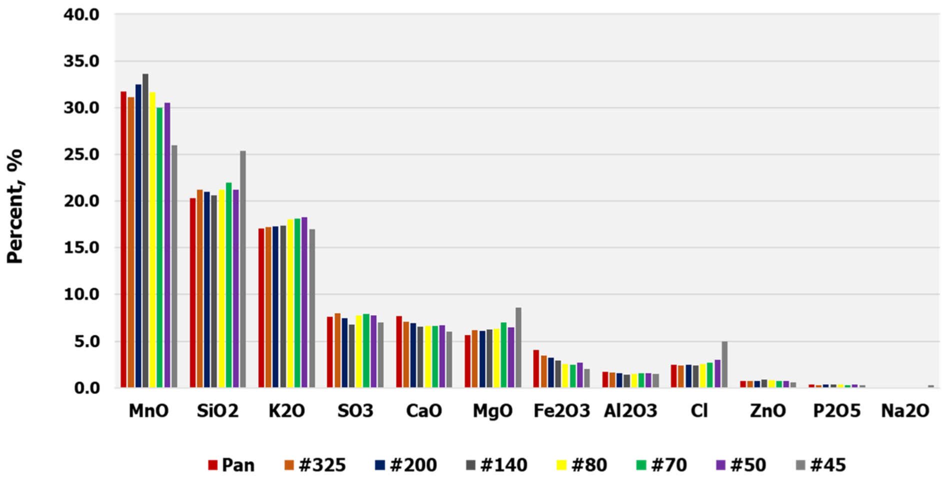

Figure 2. Elemental analysis describing the composition of the SMF-retained samples on each sieve.

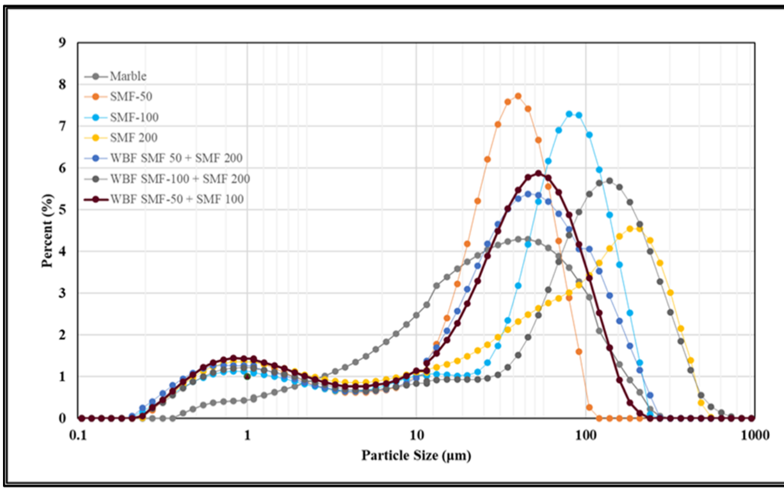

BM	PSD		
	D_{10}	D_{50}	D_{90}
Marble	5 µm	46 µm	173 µm
SMF-50	1 µm	31 µm	67 µm
SMF-100	1 µm	64 µm	168 µm
SMF-200	1 µm	54 µm	281 µm
SMF 50 + SMF 200	1 µm	42 µm	131 µm
SMF-100 + SMF 200	1 µm	94 µm	274 µm
SMF-50 + SMF 100	1 µm	36 µm	101 µm

Figure 3. PSD of SMF grades and combinations.

through different screens to acquire sized mandarin peel powder.

The existing BMs present several downsides such as prolonged processing steps of collection, drying, washing, cleaning, sieving, and packing. For example, marble is a naturally occurring material extracted from open pit mining across the world.[44] Being a naturally occurring material, marble requires several processing steps such as mining, high energy crusher, prolonged grinding, detailed sieving to acquire sized marble, and packing. In addition to that, marble raw materials also require transportation from the mining site to crushing plant and appropriate technology to carry out all operations. This study proposes a cost- and effort-effective waste material, that is, SMF that requires minor processing steps compared to other waste materials. The powdered or fumed source of the raw SMF and the presence of natural PSD make this an adequate and ready-to-use BM.

Therefore, this work aims at exploring the potential presence of particle sizes in raw SMF to be used as a BM for water-based drilling fluids. Different particle sizes were extracted from the raw SMF material and added to the water-based drilling fluid. The prepared drilling fluids were then studied for the FL test to examine the SMF impact on bridging performance, respectively. The bridging capability of the extracted SMF particles was studied against different ceramic-disc sizes using the water-based drilling fluid.

2. METHODOLOGY

2.1. Preparation of SMF. Samples of raw SMF have been collected from a local steelmaking plant and then dry-sieved. As shown in Figure 1, the sieve stack was composed of eight sieves ranging from mesh size nos. 45 to 325 and a pan. The SMF retained on mesh no. 45 was observed to have lumps and thus discarded. The remaining materials were proceeded for elemental composition analysis to examine variability in composition. The elemental analysis was conducted using X-ray fluorescence on the SMF samples retained on each mesh. The results demonstrate that SMF particles retained on each mesh is composed of oxides of manganese (31%), silicon (22%), potassium (17%), sulfur (8%), magnesium (9%), calcium (7%), iron (2%), and aluminum (2%). These oxides observed were homogeneously distributed across all the meshes (see Figure 2). Therefore, different grades of SMF samples were prepared by combining different mesh sizes together such as mesh nos. 50, 70, and 80 were combined and named as SMF-200, mesh nos. 140 and 200 were combined and named as SMF-100, and SMF-50 was prepared after combining mesh no. 325 and a pan. Subsequently, these SMF grades were further combined proportionally among each

https://doi.org/10.1021/acsomega.2c05456
ACS Omega 2023, 8, 509−518

other to explore bridging effectiveness. Figure 1 shows all the SMF grades and grade combination extracted from raw SMF. Figure 3 shows the PSD-prepared grades. It was anticipated that these natural PSD of SMF grades and grades combination would likely to plug the formation pores and hence deemed to be as effective BM for seepage losses.

As shown in Figure 3, SMF grades and their combinations observed were broadly distributed in a multimodal distribution pattern. In general, D_{10} was distributed around 1 μm, D_{50} ranged from 31 to 94 μm, and D_{90} ranged from 67 to 281 μm. The scanning electron microscopy (SEM) photomicrographs have also revealed the presence of a wide range of well-spherical and well-rounded particle sizes (Figure 4).

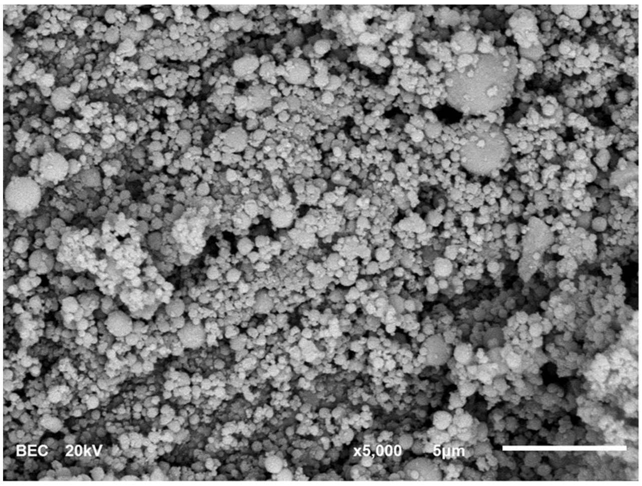

Figure 4. SEM photomicrographs of SMF.

2.2. Preparation and Testing of the SMF-Based Fluid Formulations.

Tables 1 and 2 shows composition and a battery of formulation designs using the clay-free water-based fluid (WBF) system to evaluate the bridging capacity of SMF and compared with the control, that is, marble. The WBF formulations composed of water as a base fluid, potassium chloride (inhibitive agent), sodium hydroxide (buffer), lime (hardness controller), starch (filtration controller), xanthan gum (viscosifier), polyanionic cellulose (PAC) (filtration controller), sulfonate (lubricity), and SMF and marble (bridging agent). Few drops of defoamer were added to remove the air bubbles in case of foaming. The formulations were prepared using a mixer following the API standard procedure.

Table 1. Components, Function, and Concentration of Additives Used to Prepare Water-Based Fluids

components	function	concentration
water	base fluid	0.91 bbl
potassium chloride	inhibitive agent	9.65 ppb
sodium hydroxide	buffer	0.3 ppb
lime	hardness controller	0.5 ppb
starch	filtration controller	4 ppb
xanthan gum	viscosifier	1 ppb
polyanionic cellulose	filtration controller	1.25−1.5 ppb
sulfonate	lubricity	4 ppb
SMF and marble	bridging agent	52.5 ppb

The concentration of BM was kept 15% w/v (52.5 ppb) in all WBF systems. Formulation no. 1 is a baseline formulation loaded with marble as a BM. The formulation codes 2, 3, and 4 were prepared with the SMF grades, that is, SMF-50, SMF-100, and SMF-200, respectively. In the formulation codes 5, 6, and 7, SMF grades were combined so as to maintain the total amount as 52.5 ppb. For example, 26.5 ppb of SMF-50 was combined with 26.5 ppb of SMF-200 and used in WBF-SMF system formulation code 5. Likewise, SMF-100 + SMF-200 and SMF-50 + SMF-100 were combined to prepare SMF grade combination that was used in formulation codes 6 and 7, respectively. The concept behind splitting the concentration into two-half was to examine different PSD effects on FL and FC deposition.

The high-pressure high-temperature (HPHT) filter press equipment was used with ceramic discs to study the bridging capability of the WBF system. The test simulated the formation of FC on the ceramic discs under specified testing conditions. To evaluate the performance of SMF as a BM, four different sizes of ceramic discs, that is, 10, 12, 20, and 50 μm were used under the testing conditions of 190 °F and 300 psi overbalance pressure. The FC deposited on the ceramic discs was examined and the thickness was measured in millimeters. The filtrate volume was collected after 30 min and recorded as mL/30 min. Finally, SEM was conducted on FC to investigate the internal microstructure.

3. RESULTS AND DISCUSSION

3.1. FL Behavior of SMF.

While using 10 and 12 μm ceramic discs in the HPHT filter press test, the WBF-SMF system with formulation codes 2, 3, and 4 has demonstrated an average of 46% lower filtrates compared to the reference WBF-marble system (formulation code 1), as shown in Figure 5a,b. For the 20 μm disc, all WBF-SMF systems were observed with superior FL performance compared to the WBF-marble system (Figure 5c). For example, the WBF-SMF system with formulation codes (2, 3, and 4) has shown 90, 71, and 86% lower filtrates compared to the WBF-marble system with formulation code 1, respectively. The 50 μm disc was observed with total FL for the WBF-marble system. However, the WBF-SMF system with formulation codes 2, 3, and 4 has shown 74, 59, and 70% lower filtrates against 50 μm disc compared to the WBF-marble system, respectively (Figure 5d). Accordingly, it can be inferred that all SMF grades (i.e., SMF-50, SMF-100, and SMF-200) were effective in sealing 10, 12, 20, and 50 μm ceramic discs as compared to marble.

In case of SMF-grade combination, significant improvement in sealing of ceramic discs has also been observed compared to the WBF-marble system (Figure 5). Less than 15 mL/30 min duration of FL was observed while plugging 10 and 12 μm ceramic disc for formulation codes 5, 6, and 7. For the 20 μm ceramic disc, formulation codes 5 and 7 were observed lower FL, that is, 14.5 and 14.0 mL/30 min. The formulation code 6 was observed slightly higher, that is, 18 mL/30 min. Likewise, lower FL was observed against 50 μm ceramic disc. For 50 μm ceramic discs, formulation code 7 has shown FL of 16 mL/30 min, while 5 and 6 have shown 24 and 33 mL/30 min, respectively. Overall, SMF grades and grade combination have shown remarkable bridging performance compared to marble.

In Figure 3, all the BMs, that is, SMF grades, grade combination, and marble have shown a wide range of particle size distribution. The prominent difference exists in smaller sized particle, that is, D_{10}. Approximately, in all SMF grades,

https://doi.org/10.1021/acsomega.2c05456
ACS Omega 2023, 8, 509−518

Table 2. Water-Based Fluid for Comparative Studies

WBF system	formulation code	marble (ppb)	SMF			common components
			SMF-50 (ppb)	SMF-100 (ppb)	SMF-200 (ppb)	
base WBF	1	52.5	0	0	0	0.91 bbl of water, 9.65 ppb of KCl, 0.3 ppb of NaOH, 0.5 ppb of lime, 4 ppb of starch, 1 ppb viscosifier, 1.25 ppb of polyanionic cellulose, 4 ppb of sulfonate
WBF SMF-50	2	0	52.5	0	0	
WBF SMF-100	3	0	0	52.5	0	
WBF SMF-200	4	0	0	0	52.5	
WBF SMF-50 + SMF-200	5	0	26.25	0	26.25	
WBF SMF-100 + SMF-200	6	0	0	26.25	26.25	
WBF SMF-50 + SMF-100	7	0	26.25	26.25	0	

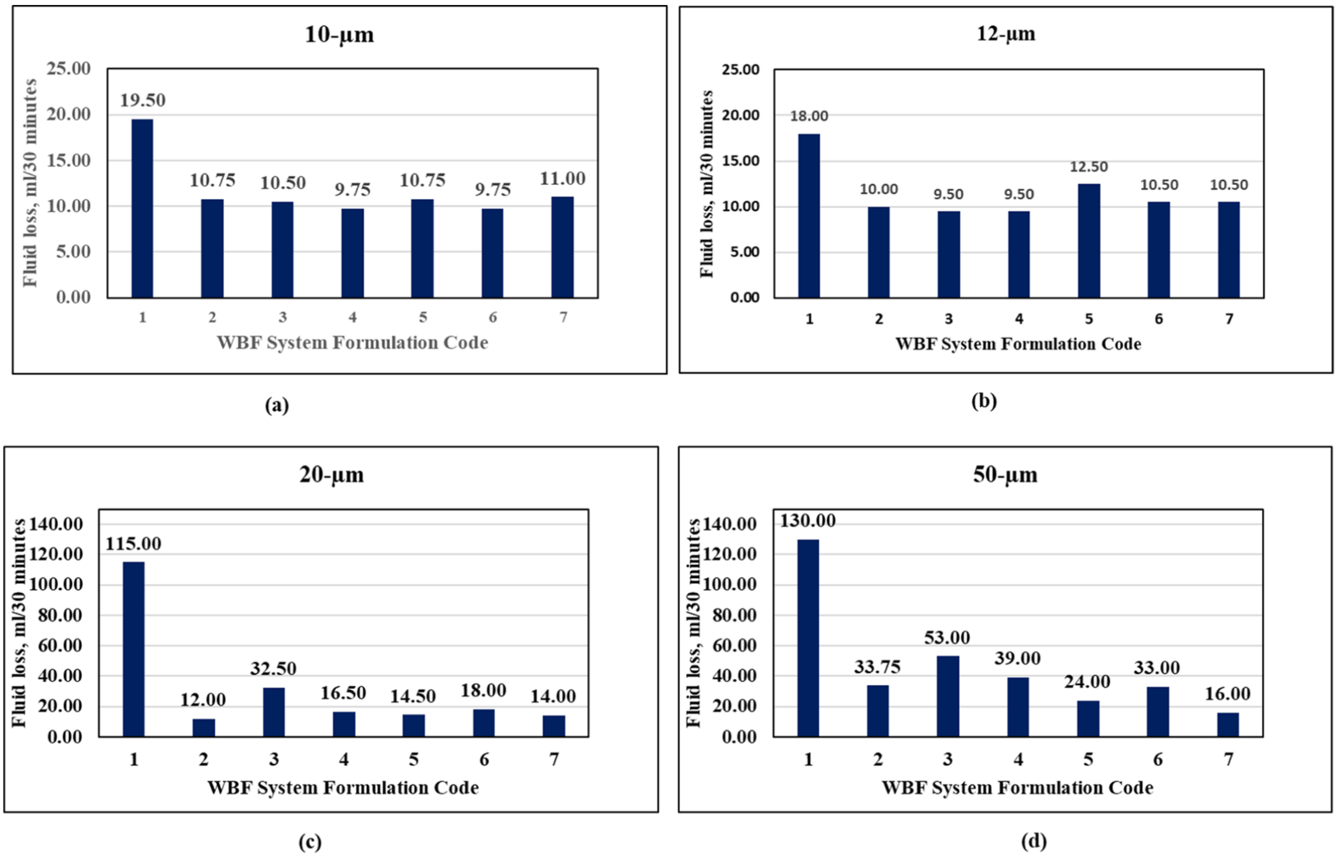

Figure 5. HPHT FL characteristics of the SMF-based fluid against (a) 10 μm ceramic disc, (b) 12 μm ceramic disc, (c) 20 μm ceramic disc, and (d) 50 μm ceramic disc under the testing conditions of 190 °F and 300 psi.

10% of the particle size is around 1 μm (i.e., D_{10} = 1 μm), whereas marble has shown D_{10} of 5 μm. The sealing capacity of marble appears to be not quite effective compared to SMF grades. In addition to that, PSD of marble is more unimodal compared to the distribution of SMF shown in Figure 3. Thus, plugging might have occurred to create an initial bridge with the large sized marble particle in formulation code 1. However, appropriate sealing is seemed to be quite negligible in marble compared to SMF. The conceivable reason behind lower FL for the WBF-SMF system against different sizes of the ceramic disc is PSD. For example, SMF grade combination used in formulation code 7 has shown a similar PSD pattern for D_{10} (i.e., D_{10} is nearly 1 μm) that has been shown in other SMF grades and their grade combination. However, the difference appears in D_{50} and D_{90}. For example, as shown in the PSD diagram (i.e., Figure 3), the D_{50} and D_{90} of SMF grade combination used in formulation code 7 were identified to be 36 and 101 μm, respectively. Similarly, formulation code 5 has also shown promising FL results against 50 μm ceramic disc. Such promising performance of formulation codes 5 and 7 is due to nearly comparable PSD and adequate amount of BM, as shown in Figure 5. The amount factor was kept constant (i.e., 52.5 ppb) in all WBF formulations. The fundamental difference appears in PSD of BMs.

In the classical FL theory, bridging, packing, and sealing mechanism occurs in a special pattern if appropriate size, shape, and amount of the BM are present in the WBF system. According to the theory, the WBF system can easily pass

https://doi.org/10.1021/acsomega.2c05456
ACS Omega 2023, 8, 509−518

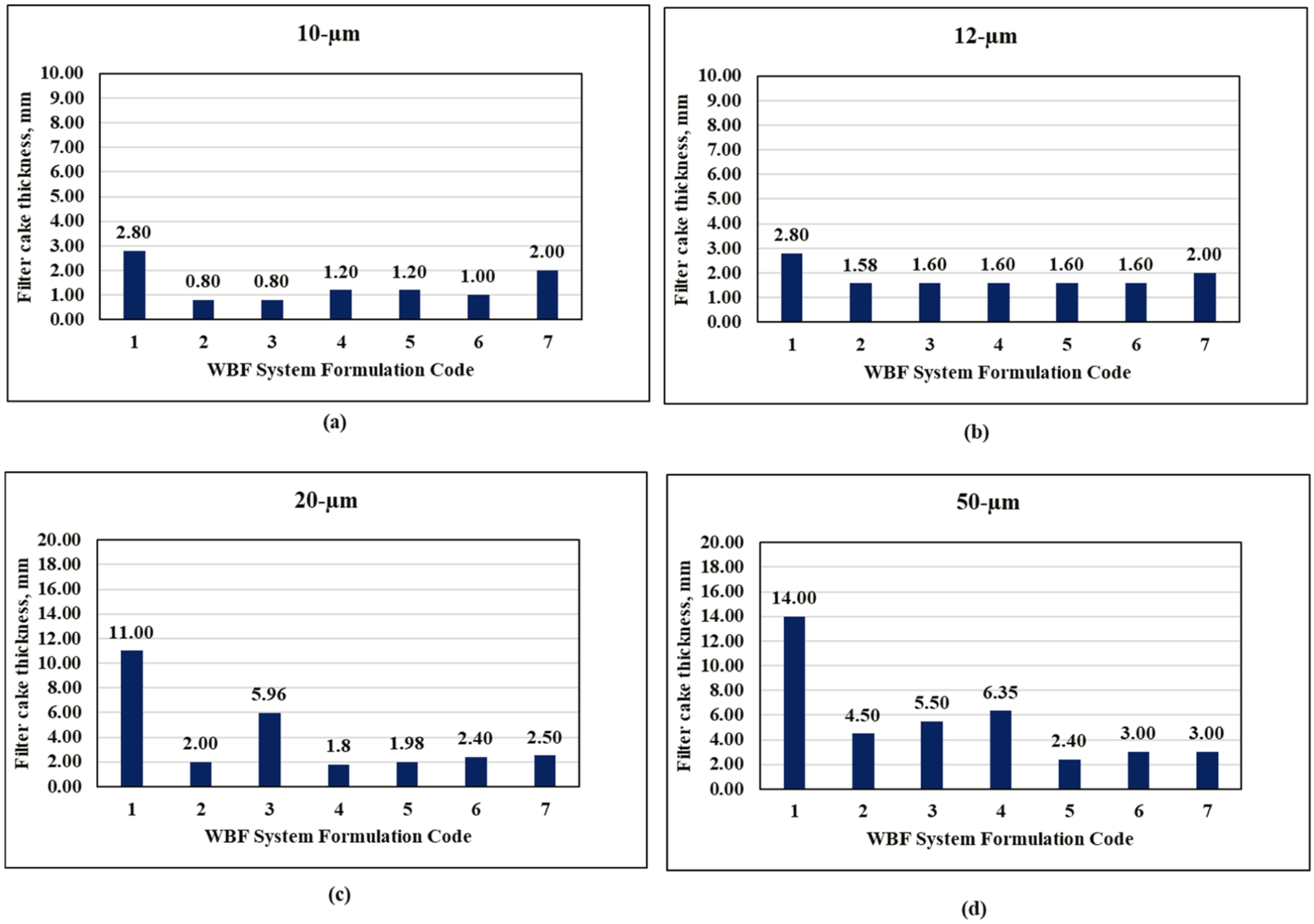

Figure 6. Evaluation of HPHT FC thickness for the WBF system against (a) 10, (b) 12, (c) 20, and (d) 50 μm ceramic discs under the testing conditions of 190 °F and 300 psi.

through porous media and result in high FL and sometimes deposit a thicker FC if smaller size and lower amount of BM are used. Therefore, no bridging and packing mechanism occurs with such smaller size particles and lesser amount of BM. Alternatively, if larger sized particles are used with higher or lower amount of BM, this will help in bridging of the pores to some extent but spaces and voids among the particles will remain open and the permeable filter will be deposited.

Jeennakorn et al. have also described that the sealing mechanism of pores is mainly driven by particle size (coarse medium and fine), shape (irregular, elongated, and their blend), and amount (40, 50, and 105 ppb) of BM.[45] The larger size particles first enter the pores and reduce the pore throat significantly, thus bridging the pore at first attempt. This bridging is further followed by the deposition of medium sized particles to further fill the pores and reduces the FL (i.e., packing). Finally, the finer particles of BMs work with the filtration control agent to fill the smaller pores present between larger and medium particles and completely seal the pores.

In the present research, SMF grades and grade combination have demonstrated the natural broader PSD and using the adequate amount of SMF (i.e., 52.5 ppb) that has been resulted in significantly controlling FL. As shown in Figure 3, the presence of broader PSD in all SMF grades and grade combination, that is, D_{10} of 1 μm, D_{50} ranging from 31 to 94 μm, and D_{90} ranging from 67 to 281 μm, has resulted in significantly lower FL compared to marble. Thus, it can be envisaged that SMF grades and grade combination have natural broader PSD that is highly likely to arrest seepage losses during drilling subterranean formation by bridging, packing, and sealing the pores in the hierarchical pattern.

3.2. FC Behavior of SMF. Figure 6 shows the FC thickness of WBF-SMF grades and grade combination and its comparison with the WBF-marble system. The WBF-SMF system has deposited significantly thinner FC on 10 and 12 μm ceramic discs compared to the WBF-marble system (Figure 6a,b). The FC deposited on 10 μm ceramic discs by the WBF-SMF system with formulation codes 2 and 3 were observed around 71% thinner, and formulation code 4 was observed around 57% thinner than the FC deposited by the WBF-marble system. In case of 20 μm, FCs deposited by the WBF-SMF system with formulation codes 2, 3, and 4 were observed 43% thinner as compared to the base WBF (Figure 6c). For the 50 μm ceramic disc, formulation codes 2, 3, and 4 have deposited 68, 61, and 55% thinner FC as compared to the WBF-marble system (Figure 6d).

The WBF system prepared from the combinations of SMF grade (i.e., formulation codes 5, 6, and 7) has demonstrated thinner FC as compared to the WBF-marble system (Figure 6). Formulation codes 5, 6, and 7 have deposited 57, 64, and 29% thinner FC on the 10 μm ceramic disc as compared to base WBF FC, respectively. In the case of 12 μm disc, formulation codes 5 and 6 have deposited 43% and

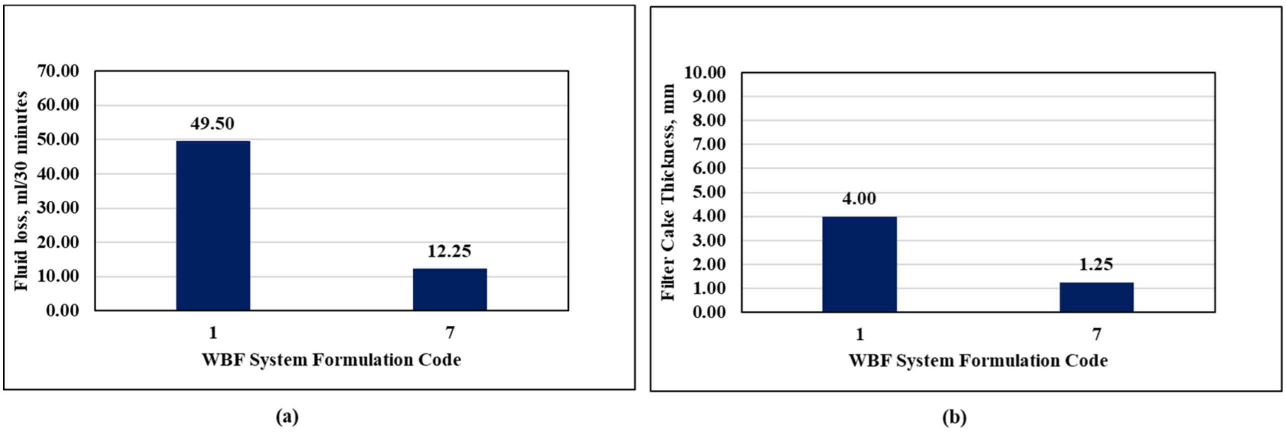

Figure 7. HPHT FL (a) and FC thickness (b) of formulation code 7 and formulation code 1 with 1.5 ppb of PAC tested against the 50 μm ceramic disc.

formulation code 7 has deposited 29% thinner FC as compared to the filter deposited by base WBF.

The FC deposited on the 20 μm ceramic disc was observed to be 82, 78, and 77% thinner in formulation codes 5, 6, and 7 as compared to the WBF-marble system, whereas as formulation codes 5, 6, and 7 have deposited 83, 79, and 79% thinner FC compared to formulation code 1 on the 50 μm ceramic disc.

FC thickness has produced surprising results when comparing formulation codes 6 and 7 with formulation code 5 for 20 and 50 μm. For 20 μm ceramic disc, formulation codes 6 and 7 have produced 2.4 and 2.5 mm of FC thickness, respectively, whereas formulation code 5 has produced 1.98 mm of FC thickness (Figure 6c). Likewise, for the 50 μm ceramic disc, formulation codes 6 and 7 have produced 3 mm of FC thickness, whereas formulation code 5 has produced 2.4 mm of FC thickness (Figure 6d). The probable reason of 0.42 to 0.60 mm thicker FC in formulation codes 6 and 7 compared to formulation code 5 is attributed to variation in PSD of SMF used in the WBF-SMF system. For instance, D_{50} and D_{90} of SMF particles used in formulation code 5 are 42 and 131 μm, those used in formulation code 6 are 94 and 274 μm, and those used in formulation code 7 are 36 and 101 μm, respectively. This variation in PSD specially at D_{50} and D_{90} is considered to be the primary reason of minor variation (i.e., 0.42 to 0.60 mm) in the FC thickness. The present research investigations are aligned with the literature. For example, Bageri et al., in 2021, have investigated that bulk volume of larger sized particles contribute to the FC thickness.[46] Therefore, variation in the D_{50} and D_{90} of formulation codes 5, 6, and 7 are the conceivable reason for minor FC variation.

Further examinations were conducted to lower the FL of the WBF-SMF system with formulation code 7, and the results were compared with the WBF-marble system with formulation code 1. To achieve this, a filtration controller, that is, PAC was slightly increased from 1.25 to 1.5 ppb in formulation codes 1 and 7. The concentration of all other chemical additives and BM were kept constant. The reason for selecting formulation code 7 for higher concentrations of PAC was its lower filtrate (i.e., 16 mL/30 min using 50 μm ceramic disc) compared to the other WBF-SMF system. Therefore, to determine the impact of partially higher PAC, two more formulations were prepared, that is, formulation code 7 and formulation code 1. Formulation code 1 was selected for comparative analysis.

As shown in Figure 7, 0.25 ppb increment of the filtration control agent, that is, from 1.25 to 1.50 ppb, has significantly reduced the FL and FC in both WBF systems. The WBF-SMF and WBF-marble systems with 1.5 PAC have 12.25 and 49.50 mL/30 min of FL against 50 μm ceramic disc. This has shown that the WBF-SMF system has produced 75% better sealing capacity compared to the WBF-marble system. It can also be deduced from this effort that SMF response to the filtration control agent appears to be positive like other BMs, that is, marble. The FC of WBF-SMF and WBF-marble systems with 1.5 PAC was 1.25 and 4 mm, respectively. Nearly 69% of thinner FC was measured in the case of the WBF-SMF system compared to the WBF-marble system. It shows that the filtration controller network provided by PAC is quite effective in reducing the FL. The enhanced network provided by 1.5 ppb of PAC helps SMF fine-sized particles (i.e., D_{10} = 1 μm) to further seal 50 μm ceramic discs pores without losing excessive fluid. Hence, lower FL deposit a thinner FC, as observed in Figure 7.

3.3. Effects of SMF PSD on Sealing Capacity. As discussed in the preceding section, Figure 3 shows the bimodal (i.e., number of two peaks) distribution of SMF grades and their combination. The first peak appears around 1 μm, and the second peak appears to be quite broadly distributed. The first peak has demonstrated relatively similar trends for all SMF grades and their grade combinations. However, the second peak of SMF grades was skewed toward a greater particle size. The SMF grade combinations have shown reasonable distribution, for example, SMF-50 + SMF 100 has shown gentle (i.e., broader) distribution of the second peak as compared to other grade combinations.

The PSD of the marble peak was observed to be unimodal (i.e., single peak) with gentle distribution. The modality or peakedness of the marble was also observed to be lower as compared to the distribution of SMF grades and grade combination. Modality (i.e., number of peaks) is one of the important parameters used to identify broad-sized particles to seal formation pores.[47,48] Savari et al.[48] have explained multi-modality or multi-modal as broad PSD with peaks at a number of size intervals.

For example, as can be seen in Figure 3, SMF grades and grade combination identified peaks around 1 and 75 μm. These PSD data indicate natural bimodal distribution of SMF at intervals of two different sizes. This was potentially deemed to be effective in sealing 10, 12, 20, and 50 μm ceramic discs as compared to the unimodal distribution of the marble.

According to the FL theory, the bridging, packing, and sealing mechanism starts with larger sized particles, followed by medium and finer particles. Following these theories, such a plugging mechanism has produced lesser FL and thinner FC. Likewise, multi-modal PSD of SMF and SMF grade combination has produced lesser FL and FC compared to the marble.

Thus, it could be believed that the larger particle of SMF enters the formation pores first and creates an initial bridge, followed by finer particles, to completely seal the FC. Figure 8 shows the SEM photomicrograph of FC deposited from the WBF-SMF system. The SEM images were taken from the cross-sectional view of the FC. From the morphological view, the FC appears to be non-porous, that is, impermeable. The photomicrographs also confirm the presence of the wide range of particles present in the FC.

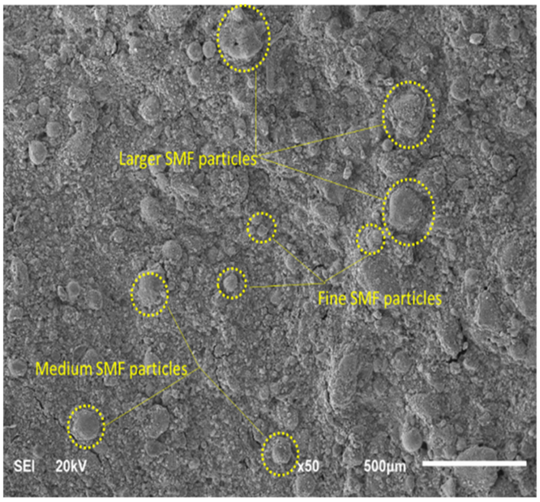

Figure 8. SEM photomicrograph of FC generated from the WBF-SMF system at a resolution of 500 μm.

Further examination was conducted to examine the FC at higher resolution (i.e., 5 μm). Figure 9 shows that in addition to larger, medium, and fine particles, there are a reasonable amount of finer particles present in the FC. These finer particles of SMF are deeply engraved into the FC, thus providing the sealing mechanism. Therefore, lower FL and thinner FC were observed in WBF-SMF systems, as shown in Figures 4 and 7.

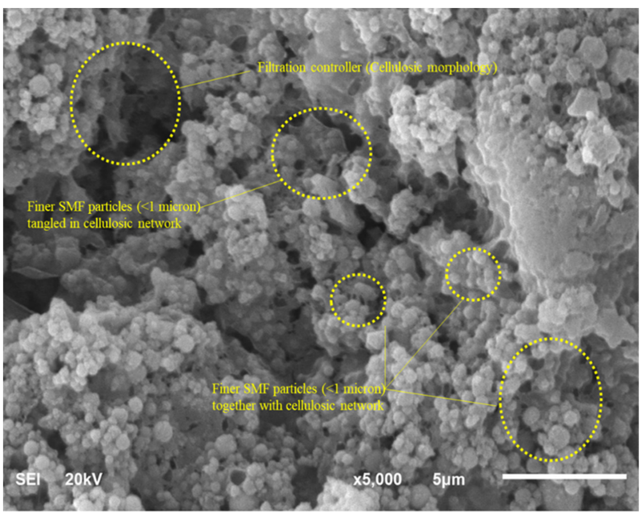

Figure 9. SEM photomicrograph of FC generated from the WBF-SMF system at a resolution of 5 μm.

As depicted in Figure 9, finer particles are tangled in between the filtration controller (i.e., polyanionic cellulosic layers). Such cellulosic layers are providing foundation for BM to completely seal the pores. Thus, SEM findings confirm the effective sealing capacity of SMF. The SEM image of FC generated from the WBF-SMF system at a higher resolution also reveals the presence of SMF of particle size smaller than 1 μm. Such finer particles of SMF present in the FC can also be identified from PSD result, as demonstrated in Figure 3. Thus, SMF has exhibited significantly improved performance against ceramics discs, and it can be effectively used in bridging and sealing pores encountered during seepage losses.

4. CONCLUSIONS

A novel granular type BM from waste origin was investigated in this study in the presence of water-based drilling fluid. Several grades were extracted from the raw waste SMF. The main findings of this study are as follows:

- Experiments have demonstrated that SMF poses a unique PSD of D_{10} 1 μm, D_{50} ranging between 31 and 94 μm, and D_{90} ranging between 67 and 281 μm. The morphology is predominantly well-rounded and of well-spherical nature.
- The filtration properties using HPHT filter press experiment system at 190 °F and 300 psi have shown that the addition of SMF to WBF has substantially enhanced the filtration performance compared to the WBF-marble system, which has been taken as a reference. In fact, SMF was found to be the best candidate to plug a wide range of pore sizes ranging from 10 to 50 μm.
- On average, FL for SMF grades significantly decreased by 47, 46, 82, and 68% for 10, 12, 20, and 50 μm ceramic discs with respect to baseline, respectively. The SMF grade combination has demonstrated 46, 37, 86, and 81% for 10, 12, 20, and 50 μm ceramic discs with respect to baseline, respectively.
- This research has investigated SMF as an economical, effortless, readily available, and high-performance material that demonstrates bridging, packing, and sealing mechanism of the pores.

Though the SMF performance is promising, the present study is limited to the WBF system at 190 °F and 300 psi. It is recommended to determine SMF performance in different mud systems (e.g., oil-based mud) and more challenging environments such as high density and high temperature. In addition, a detailed cost analysis is also recommended to determine SMF processing cost.

■ AUTHOR INFORMATION

Corresponding Author

Salaheldin Elkatatny − *College of Petroleum Engineering and Geosciences, King Fahd University of Petroleum and Minerals, 31261 Dhahran, Saudi Arabia;* orcid.org/0000-0002-7209-3715; Phone: +966-594663692; Email: elkatatny@kfupm.edu.sa

Authors

Waseem Razzaq − *University of Technology Malaysia, 81310 Johor Bahru, Johor, Malaysia*

Ahmed Gowida − *College of Petroleum Engineering and Geosciences, King Fahd University of Petroleum and Minerals, 31261 Dhahran, Saudi Arabia*

Ariffin Samsuri − *University of Technology Malaysia, 81310 Johor Bahru, Johor, Malaysia*

Complete contact information is available at: https://pubs.acs.org/10.1021/acsomega.2c05456

Author Contributions

Conceptualization, A.S. and W.R.; methodology, W.R.; formal analysis, W.R.; conducting experiments, W.R.; resources, A.S.; data analysis, W.R.; writing—original draft preparation, W.R.; writing—review and editing, S.E. and A.G.; visualization, W.R., and A.G.; supervision, S.E.; all authors have read and agreed to the published version of the manuscript.

Notes

The authors declare no competing financial interest.

■ ACKNOWLEDGMENTS

The authors would like to acknowledge University Technology Malaysia and King Fahd University of Petroleum and Minerals for allowing the publication of this article.

■ NOMENCLATURE

SMF, silicomanganese fume
WBF, water-based drilling fluid
API, American Petroleum Institute
XRF, X-ray fluorescence
SEM, scanning electron microscopy
EDX, energy dispersive X-ray
HPHT, high-pressure high-temperature
GS, gel strength
PV, plastic viscosity
YP, yield point
RPM, revolution per minutes
BHR, before hot rolling
AHR, after hot rolling
w/v, weight by volume
D_{10}, particle size corresponds to 10% cumulative
D_{50}, particle size corresponds to 50% cumulative
D_{90}, particle size corresponds to 90% cumulative

■ REFERENCES

(1) Nath, S. K.; Randhawa, N. S.; Kumar, S. A review on characteristics of silico-manganese slag and its utilization into construction materials. *Resour., Conserv. Recycl.* **2022**, *176*, 105946.

(2) Chakravarty, T.; Panigrahi, S. Strategies for solid waste management in SAIL steel plants. *Proceedings: NS-EWM*, 1996.

(3) Arnoldussen, Y. J.; Kringlen Ervik, T.; Samulin Erdem, J.; Kero, I.; Baarnes Eriksen, M.; Skaug, V.; Zienolddiny, S. Mechanisms of Toxicity of Industrially Relevant Silicomanganese Dust on Human 1321N1 Astrocytoma Cells: An In Vitro Study. *Int. J. Mol. Sci.* **2019**, *20*, 740.

(4) Frías, M.; Rodríguez, C. Effect of incorporating ferroalloy industry wastes as complementary cementing materials on the properties of blended cement matrices. *Cem. Concr. Compos.* **2008**, *30*, 212−219.

(5) Ma, Y.; Kero, I.; Tranell, G. Fume Formation from Oxidation of Liquid SiMn Alloy. *Oxid. Met.* **2018**, *89*, 211−231.

(6) Najamuddin, S. K.; Megat Johari, M. A.; Maslehuddin, M.; Yusuf, M. O. Synthesis of low temperature cured alkaline activated silicomanganese fume mortar. *Constr. Build. Mater.* **2019**, *200*, 387−397.

(7) Nasir, M.; Johari, M. A. M.; Maslehuddin, M.; Yusuf, M. O.; Al-Harthi, M. A. Influence of heat curing period and temperature on the strength of silico-manganese fume-blast furnace slag-based alkali-activated mortar. *Constr. Build. Mater.* **2020**, *251*, 118961.

(8) Nasir, M.; Megat Johari, M. A.; Yusuf, M. O.; Maslehuddin, M.; Al-Harthi, M. A.; Dafalla, H. Impact of Slag Content and Curing Methods on the Strength of Alkaline-Activated Silico-Manganese Fume/Blast Furnace Slag Mortars. *Arabian J. Sci. Eng.* **2019**, *44*, 8325−8335.

(9) Navarro, R.; Zornoza, E.; Garcés, P.; Sánchez, I.; Alcocel, E. G. Optimization of the alkali activation conditions of ground granulated SiMn slag. *Constr. Build. Mater.* **2017**, *150*, 781−791.

(10) Steenkamp, J. D.; Sutherland, J. J.; Hayman, D. A.; Muller, J. Tap-Hole Life Cycle Design Criteria: A Case Study Based on Silicomanganese Production. *JOM* **2016**, *68*, 1547−1555.

(11) Frías, M.; Sánchez de Rojas, M. S.; Menéndez, I.; de Lomas, M. G.; Rodríguez, C. Properties of SiMn slag as apozzolanic material in portland cement manufacture. *Mater. Constr.* **2005**, *55*, 53−62.

(12) Morone, M.; Costa, G.; Polettini, A.; Pomi, R.; Baciocchi, R. Valorization of steel slag by a combined carbonation and granulation treatment. *Miner. Eng.* **2014**, *59*, 82−90.

(13) Gao, J.; Sha, A.; Wang, Z.; Tong, Z.; Liu, Z. Utilization of steel slag as aggregate in asphalt mixtures for microwave deicing. *J. Cleaner Prod.* **2017**, *152*, 429−442.

(14) Shen, R.; Zhang, G.; Dell'Amico, M.; Brown, P.; Ostrovski, O. A feasibility study of recycling of manganese furnace dust. *INFACON XI*, 2007.

(15) Fink, J. Chapter 1—Drilling muds. In *Petroleum Engineer's Guide to Oil Field Chemicals and Fluids*, 3rd ed.; Fink, J., Ed.; Gulf Professional Publishing, 2021; pp 1−122.

(16) Gudarzifar, H.; Sabbaghi, S.; Rezvani, A.; Saboori, R. Experimental investigation of rheological & filtration properties and thermal conductivity of water-based drilling fluid enhanced. *Powder Technol.* **2020**, *368*, 323−341.

(17) Fink, J. Chapter 2—Fluid loss additives. In *Petroleum Engineer's Guide to Oil Field Chemicals and Fluids*, 3rd ed.; Fink, J., Ed.; Gulf Professional Publishing, 2021; pp 123−202.

(18) He, W.; Hayatdavoudi, A.; Chen, K.; Sawant, K.; Zhang, Q.; Zhang, C. Enhancement of Plastering Effect on Strengthening Wellbore by Optimizing Particle Size Distribution of Wellbore Strengthening Materials. *J. Energy Resour. Technol.* **2019**, *141*, 122905.

(19) Elkatatny, S.; Mahmoud, M.; Nasr-El-Din, H. A. Filter Cake Properties of Water-Based Drilling Fluids Under Static and Dynamic Conditions Using Computed Tomography Scan. *J. Energy Resour. Technol.* **2013**, *135*, 042201.

(20) Adewole, J. K.; Najimu, M. O. A Study on the Effects of Date Pit-Based Additive on the Performance of Water-Based Drilling Fluid. *J. Energy Resour. Technol.* **2018**, *140*, 052903.

(21) Howard, G.; Fast, C. *Hydraulic Fracturing*; Monograph Series; Society of Petroleum Engineers of AIME: Richardson, TX, 1970; Vol. 2, p 34.

(22) Navarrete, R. C.; Cawiezel, K. E.; Constien, V. G. Dynamic Fluid Loss in Hydraulic Fracturing Under Realistic Shear Conditions in High-Permeability Rocks. In *SPE Annual Technical Conference and Exhibition*, 1994.

(23) Darley, H. C. H. Designing Fast Drilling Fluids. *J. Pet. Technol.* **1965**, *17*, 465−470.

(24) Elkatatny, S.; Ahmed, A.; Abughaban, M.; Patil, S. Deep Illustration for Loss of Circulation While Drilling. *Arabian J. Sci. Eng.* **2020**, *45*, 483−499.

(25) Al-Hameedi, A. T.; Alkinani, H. H.; Dunn-Norman, S.; Flori, R. E.; Hilgedick, S. A.; Amer, A. S.; Alsaba, M. T. Using Machine Learning to Predict Lost Circulation in the Rumaila Field, Iraq. In *SPE Asia Pacific Oil and Gas Conference and Exhibition*, 2018.

(26) Amanullah, M.; Ramasamy, J.; Al-Arfaj, M. K.; Aramco, S. Application of an indigenous eco-friendly raw material as fluid loss additive. *J. Pet. Sci. Eng.* **2016**, *139*, 191−197.

(27) Musaed, N. J. A.; Fattah, K. A. Utilization of shredded waste car tyres as a fracture seal material (FSM) in oil and gas drilling operations. *J. Pet. Gas Eng.* **2017**, *8*, 21−28.

(28) Ramasamy, J.; Amanullah, M. Novel Fibrous Lost Circulation Materials Derived from Deceased Date Tree Waste. In *SPE Kingdom of Saudi Arabia Annual Technical Symposium and Exhibition*, 2017.

(29) Sauki, A.; Hasan, N. I.; Naimi, F. B. M.; Othman, N. H. Development of environmental friendly lost circulation material from banana peel. In *AIP Conference Proceedings*; AIP Publishing LLC, 2017; p 130016.

(30) Wajheeuddin, M.; Hossain, M. E. Development of an Environmentally-Friendly Water-Based Mud System Using Natural Materials. *Arabian J. Sci. Eng.* **2017**, *43*, 2501−2513.

(31) Fadliah, F.; Manan, H.; Hamid, A.; Pratiwi, R.; Fajarwati, K. Utilization of styrofoam waste as a lost circulation material in drilling mud. *J. Phys.: Conf. Ser.* **2019**, *1402*, 033005.

(32) Fatihah Majid, N. F.; Katende, A.; Ismail, I.; Sagala, F.; Sharif, N. M.; Che Yunus, M. A. A comprehensive investigation on the performance of durian rind as a lost circulation material in water based drilling mud. *Petroleum* **2019**, *5*, 285−294.

(33) Idress, M.; Hasan, M. L. Investigation of different environmental-friendly waste materials as lost circulation additive in drilling fluids. *J. Pet. Explor. Prod. Technol.* **2019**, *10*, 233−242.

(34) Agwu, O. E.; Akpabio, J. U.; Akpabio, M. G. Potentials of waste seashells as additives in drilling muds and in oil well cements. *Cleaner Eng. Technol.* **2020**, *1*, 100008.

(35) Nik Ab Lah, N. K. I.; Ngah, K.; Sauki, A. Study on the viability of egg shell as a lost circulation material in synthetic based drilling fluid. *J. Phys.: Conf. Ser.* **2019**, *1349*, 012135.

(36) Al-Hameedi, A. T. T.; Alkinani, H. H.; Albazzaz, H. W.; Dunn-Norman, S.; Alkhamis, M. M. Insights into the applications of waste materials in the oil and gas industry: State of the art review, availability, cost analysis, and classification. *J. Pet. Explor. Prod. Technol.* **2020**, *10*, 2137−2151.

(37) Al-Hameedi, A. T. T.; Alkinani, H. H.; Alkhamis, M. M.; Dunn-Norman, S. Utilizing Food Waste Product (Date Tree Seeds) to Enhance the Filtration Characteristics in Water-Based Drilling Fluid System: A Comparative Study. *J. Energy Resour. Technol.* **2020**, *142*, 123201.

(38) Amanullah, M.; Alouhali, R.; AlArfaj, M. A Date Tree Fiber-Based LCM for Severe Loss Control. In *International Petroleum Technology Conference*; OnePetro, 2020.

(39) Sauki, A.; Azmi, M. S. M.; Jarni, H. H.; Bakar, W. Z. W.; Mohd, T. A. T.; Lah, N. K. I. N. A.; Khamaruddin, P. N. F. M.; Ibrahim, W. A. Feasibility Study of using Oil Palm Trunk Waste Fiber as Fluid Loss Control Agent and Lost Circulation Material in Drilling Mud. *J. Adv. Res. Fluid Mech. Therm. Sci.* **2020**, *72*, 9−20.

(40) Rita, N.; Khalid, I.; Efras, M. R. Rheological Properties of Drilling Mud Consist of CMC Which is Made by Carton Waste and Chemical Additive of Na2CO3 for Reducing Lost Circulation. *IOP Conf. Ser.: Mater. Sci. Eng.* **2020**, *884*, 012027.

(41) Sedaghatzadeh, M.; Shahbazi, K.; Pourafshary, P.; Razavi, S. A. Experimental investigation of the application of Eucalyptus bark to prevent lost circulation in pay zones with acid dissolution capability. *Petroleum* **2021**, *7*, 152−159.

(42) Medved, I.; Gaurina-Međimurec, N.; Pašić, B.; Mijić, P. Green Approach in Water-Based Drilling Mud Design to Increase Wellbore Stability. *Appl. Sci.* **2022**, *12*, 5348.

(43) Medved, I.; Gaurina-Međimurec, N.; Novak Mavar, K.; Mijić, P. Waste Mandarin Peel as an Eco-Friendly Water-Based Drilling Fluid Additive. *Energies* **2022**, *15*, 2591.

(44) Harvey, C. *Resources, Applications and Market Trends of Calcium Carbonates in the Northern Pacific Rim*; British Columbia Geological Survey, 1995; p 101.

(45) Jeennakorn, M.; Alsaba, M.; Nygaard, R.; Saasen, A.; Nes, O.-M. The effect of testing conditions on the performance of lost circulation materials: understandable sealing mechanism. *J. Pet. Explor. Prod. Technol.* **2019**, *9*, 823−836.

(46) Bageri, B. S.; Adebayo, A. R.; Al Jaberi, J.; Patil, S.; Salin, R. B. Evaluating drilling fluid infiltration in porous media—Comparing NMR, gravimetric, and X-ray CT scan methods. *J. Pet. Sci. Eng.* **2021**, *198*, 108242.

(47) Nguyen, K.; Mehrabian, A.; Santra, A. Multi-modal particle size distribution of lost circulation material blend for controlling fluid losses from multiple fractures around inclined wellbores. In *SPE Asia Pacific Oil and Gas Conference and Exhibition*; OnePetro, 2020.

(48) Savari, S.; Whitfill, D. L.; Walker, J. Lost circulation management in naturally fractured reservoirs. In *SPE/IADC Middle East Drilling Technology Conference and Exhibition*; OnePetro, 2016.